Gray Spectralon polarized reflectance deviations from Lambertian

Nathaniel Field, Jarrod Brown, Darrel Card, Chad Welsh, Andre Van Rynbach, et al.

Nathaniel J. Field, Jarrod P. Brown, Darrel B. Card, Chad M. Welsh, Andre J. Van Rynbach, Joseph A. Shaw, "Gray Spectralon polarized reflectance deviations from Lambertian," Proc. SPIE 12112, Polarization: Measurement, Analysis, and Remote Sensing XV, 121120A (3 June 2022); doi: 10.1117/12.2618868

SPIE.

Event: SPIE Defense + Commercial Sensing, 2022, Orlando, Florida, United States

Gray Spectralon polarized reflectance deviations from Lambertian

Nathaniel J. Field[1], Jarrod P. Brown[2], Darrel B. Card[2], Chad M. Welsh[2],
Andre J. Van Rynbach[3], Joseph A. Shaw[1,4]
[1] *Electrical & Computer Engineering, Montana State University, Bozeman, MT, USA*
[2] *Air Force Research Lab, Munitions Directorate, Eglin AFB, FL, USA*
[3] *Air Force Research Lab, LADAR Technology Branch, WPAFB, OH, USA*
[4] *Optical Technology Center, Montana State University, Bozeman, MT, USA*

Abstract

While Spectralon panels are largely assumed to be ideal Lambertian surfaces, their actual polarized reflective responses deviate from the ideal by at least a small amount at illumination and viewing angles off surface normal. The Mueller matrix response of four different panels between 10% and 99% reflectance were measured and the radiometric response from two distinct monostatic or near-monostatic polarimeter systems are compared, one at Montana State University and one at the Air Force Research Lab. The deviations from an assumed ideal Lambertian surface are reported.

1. Introduction and Background

Spectralon® and other similar sintered polytetrafluoroethylene (PTFE) diffuse reflectors are reflectance standards commonly used for radiometric calibrations. The undoped, white 99% reflective panel has well-studied properties. Gray-scale versions are useful options when calibrating remote sensing systems which are likely to target or observe less reflective diffuse surfaces, such as autonomous vehicles likely to see pedestrians in darker clothes.

Current research at Montana State University (MSU) and the Air Force Research Labs (AFRL) has interest in quantifying the polarimetric and radiometric response of gray Spectralon for calibration purposes, particularly in the monostatic (or near-monostatic) geometries. While there has been continued research into the Spectralon spectropolarimetric response, they have focused on limited illumination or viewing geometries [1–3], considered only white Spectralon [4–6], or ignored the monostatic geometries [7,8]. The increasingly non-Lambertian nature of darker doped PTFE panels has been noted for decades [9], but the monostatic case is still not well-studied.

The MSU team used a near-monostatic Mueller lidar test-bed to collect the monostatic case of the full Mueller matrix bidirectional reflectance distribution function (P-mBRDF). In addition to these polarimetric data discussions, the unpolarized radiometric responses were compared to data collected by the AFRL using a novel monostatic device described in [10].

2. Devices

2.1 MSU Mueller Lidar Test-Bed

The Mueller lidar uses the same polarizer and retarder arrangement and the analysis methods described in this group's previous work [11]. The laser has simultaneous 532 nm and 1064 nm outputs along the same optical path. The receiver includes a 1064 nm laser-line filter, so only the near infrared illumination is received. All measurements in this research are made with 619.2 μJ pulse energy, 7 ns FWHM pulse width, and 20 Hz pulse repetition frequency. The sensor-target

Polarization: Measurement, Analysis, and Remote Sensing XV, edited by David B. Chenault,
Meredith K. Kupinski, Proc. of SPIE Vol. 12112, 121120A · © 2022 SPIE
0277-786X · doi: 10.1117/12.2618868

distance is 1.575 m, the beam diameter at the target is 8 mm, and the receiver field-of-view is 1.13° (full angle). The sensor is therefore in an underfilled-FOV configuration.

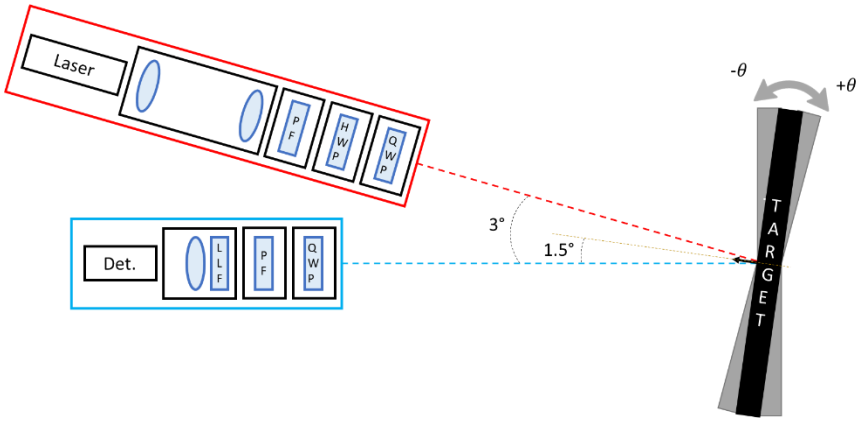

Figure 1. Exaggerated angular geometry of the Mueller lidar test-bed. A 0° incidence/viewing angle is defined when the surface normal of the target is 1.5° from the optical paths of both the transmitter and the receiver.

Although this lidar is not strictly monostatic, the approximate 3° separation between the transmitter and receiver is a much smaller transmitter-receiver separation angle than any of those in the other studies which measure the BRDF of gray Spectralon [3–5,7,8].

2.2 AFRL Temporally-Multiplexed Polarimetric Ladar

The AFRL data were collected using the novel temporally-multiplexed polarimetric lidar (TMP-LADAR). This ladar also operates at 1064 nm, but it is fully monostatic and has a 10 ns FWHM pulse width and 10 kHz pulse repetition frequency.

3. Experimental Results and Discussion

3.1 Unpolarized Radiometric Response

Although both measurement systems have polarized transmitters and receivers, the unpolarized response can be pulled from the Mueller matrices from the m_{00} coefficient. Both the MSU and AFRL groups were able to measure the output powers from their transmitters, allowing us to report the absolute reflectance values and directly calculate the monostatic BRDF. The summary of these absolute measurements is shown in Fig. 2.

The equation used to calculate the BRDF from the individual measurements is:

$$BRDF(\theta) = \frac{V_{meas}}{V_{tot}} * \frac{1}{\Omega * \cos(\theta)} \quad (1)$$

Where V_{meas} is the received signal voltage, V_{tot} is the received signal voltage when the transmitter is fired directly into the receiver, Ω is the receiver solid angle, and θ is the angle of the target surface normal with respect to the device's optical paths.

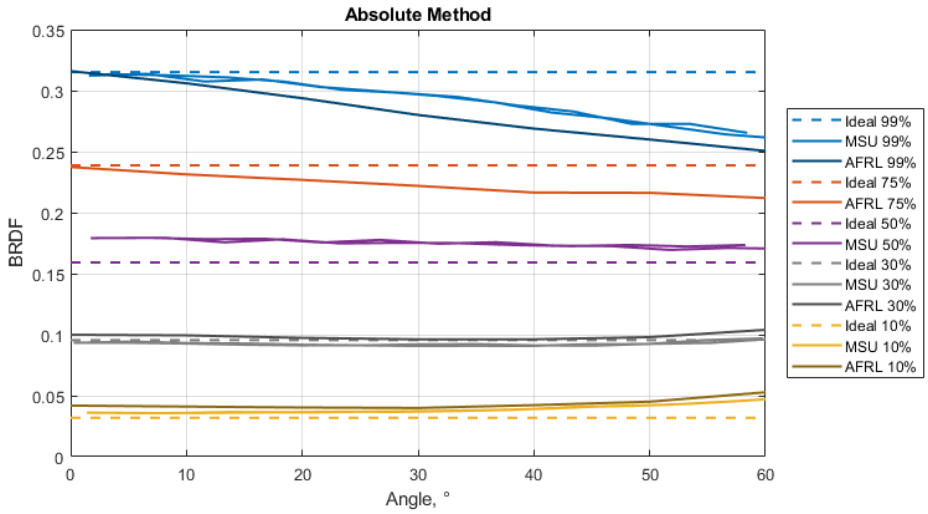

Figure 2. Summary of Spectralon monostatic BRDF measurements as compared to the ideal for a Lambertian surface of each panels' nominal reflectance, using the absolute method of BRDF calculation.

Both groups also used a second reference method, validating the reference method as an option for future work when direct measurement of the transmitter beam cannot be easily accomplished. This method uses only the normal incidence signal from the 99% panel; this is the most Lambertian panel and geometry combination. The reference method uses the following equation instead:

$$BRDF(\theta) = \frac{V_{meas}}{V_{ref}} * \frac{0.99}{\pi * \cos(\theta)} \tag{2}$$

Where V_{ref} is the received signal voltage for the 99% panel at 0° incidence with otherwise similar device parameters as those used for the latter V_{meas} values. This method produced the results summarized in Fig. 3, which are notably incredibly similar to those using the absolute method.

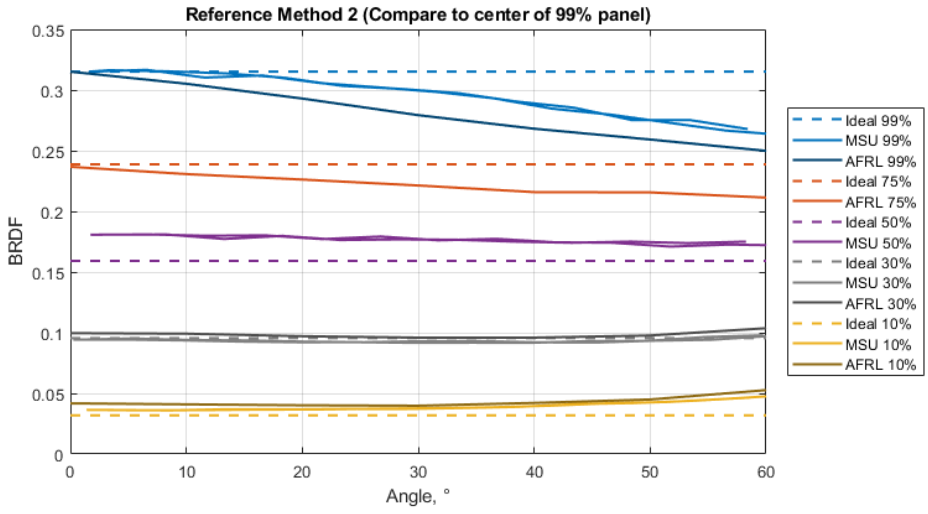

Figure 3. Summary of Spectralon monostatic BRDF measurements as compared to the ideal for a Lambertian surface of each panels' nominal reflectance, using the reference method of BRDF calculation.

The BRDF values for these monostatic geometries are actually closer to ideal for lower reflectance panels than higher, unlike that which has been found for other geometries in previous research. The RMS errors from the ideal Lambertian BRDF for the MSU measurements of 99%, 50%, 30%, and 10% panels were 0.029, 0.016, 0.003, and 0.008, respectively. For the AFRL measurements, the RMS errors for the panels, in descending order of reflectance, were 0.043, 0.064, 0.008, and 0.017. The AFRL was able to take directional hemispheric radiance (DHR) measurements for the 30% and 10% panels measured by both groups. Using these more specific DHR values in place of the nominal reflectance values of the panels, the average RMS error for the MSU and AFRL measurements for the 30% and 10% panels were 0.014 and 0.007. The 50% Spectralon panel is an interesting case because it is quite consistent over incidence angles but consistently above the ideal Lambertian value. If we treat it instead as a 55% reflective panel, the RMS error is only 0.003.

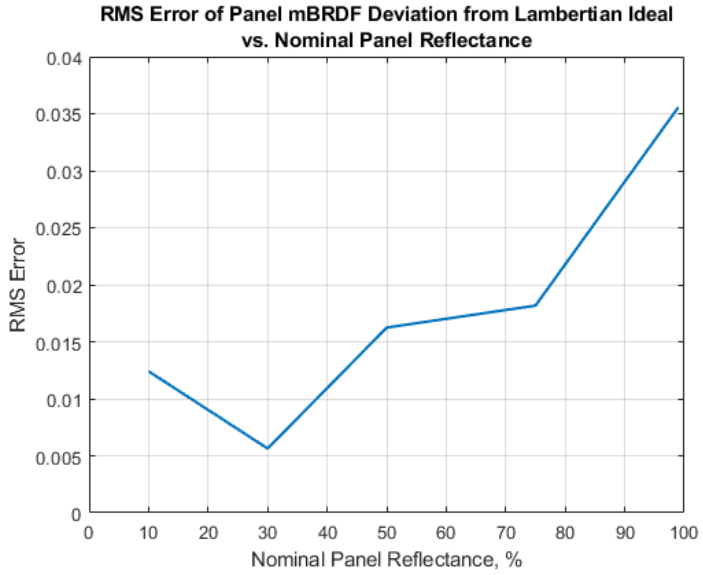

Figure 4. Average RMS error of MSU and AFRL mBRDF measurements as compared to the expected ideal Lambertian mBRDF for the panels' nominal reflectance values.

Qualitatively, high-reflectance panels show the mBRDF falling below the ideal as the incidence angle increases; but low-reflectance panels show the opposite, with mBRDF increasing above the ideal with increasing incidence angle.

3.2 Polarimetric Characteristics

The Mueller matrix mBRDF values are presented here for the 99%, 50%, 30%, and 10% panels measured by the MSU device. The approximate Lambertian reflectance (the mBRDF value multiplied by π) is reported in place of the m_{00} coefficients, which are all normalized to 1. The other 15 coefficients are normalized by the m_{00} coefficient.

Each of the Mueller mBRDF coefficients reported here are the averaged values of multiple measurement sets viewing different areas of the same panels. The maximum deviation of the presented average values is ±2.5%.

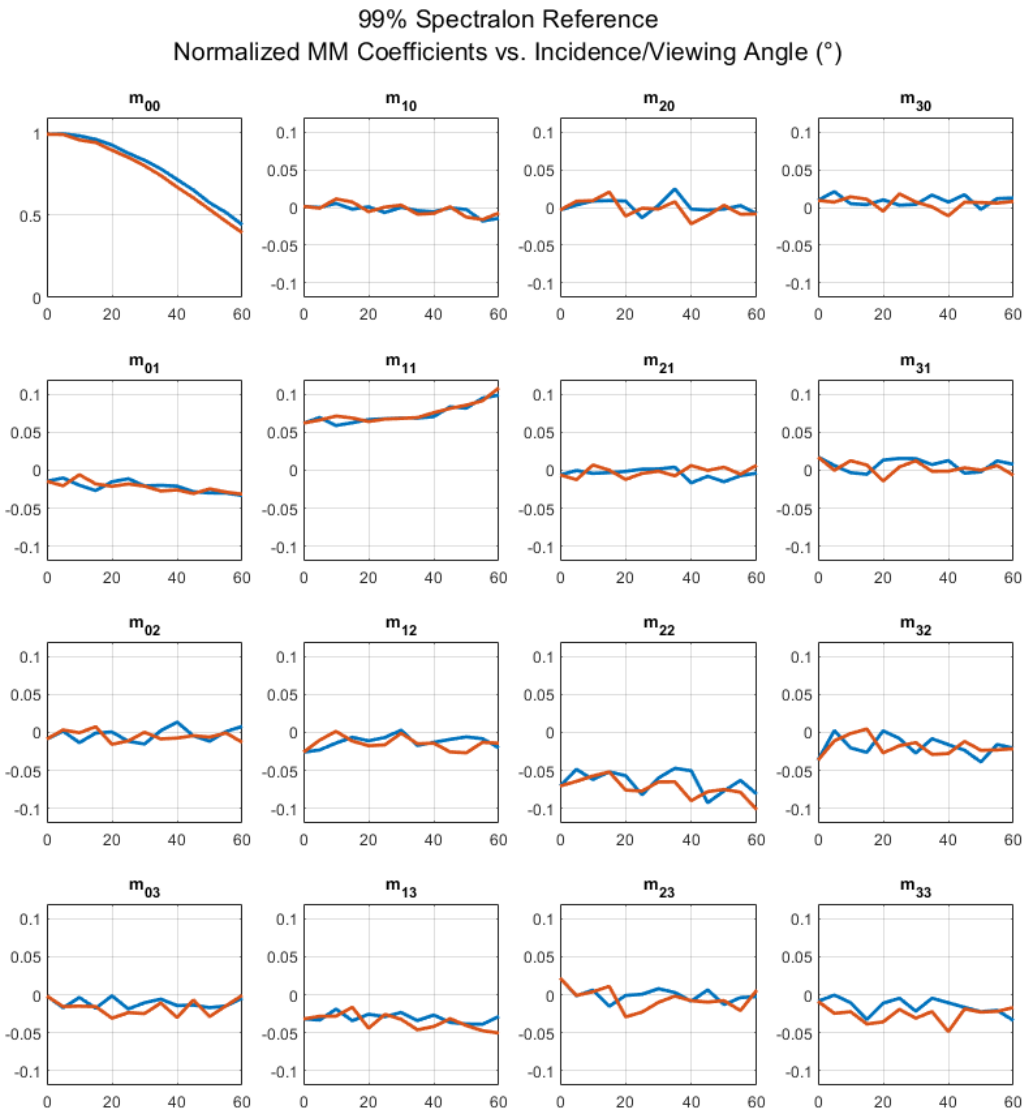

Figure 5. Mueller matrix mBRDF for a 99% Spectralon panel. The blue lines denote negative angles, and the red lines denote positive angles.

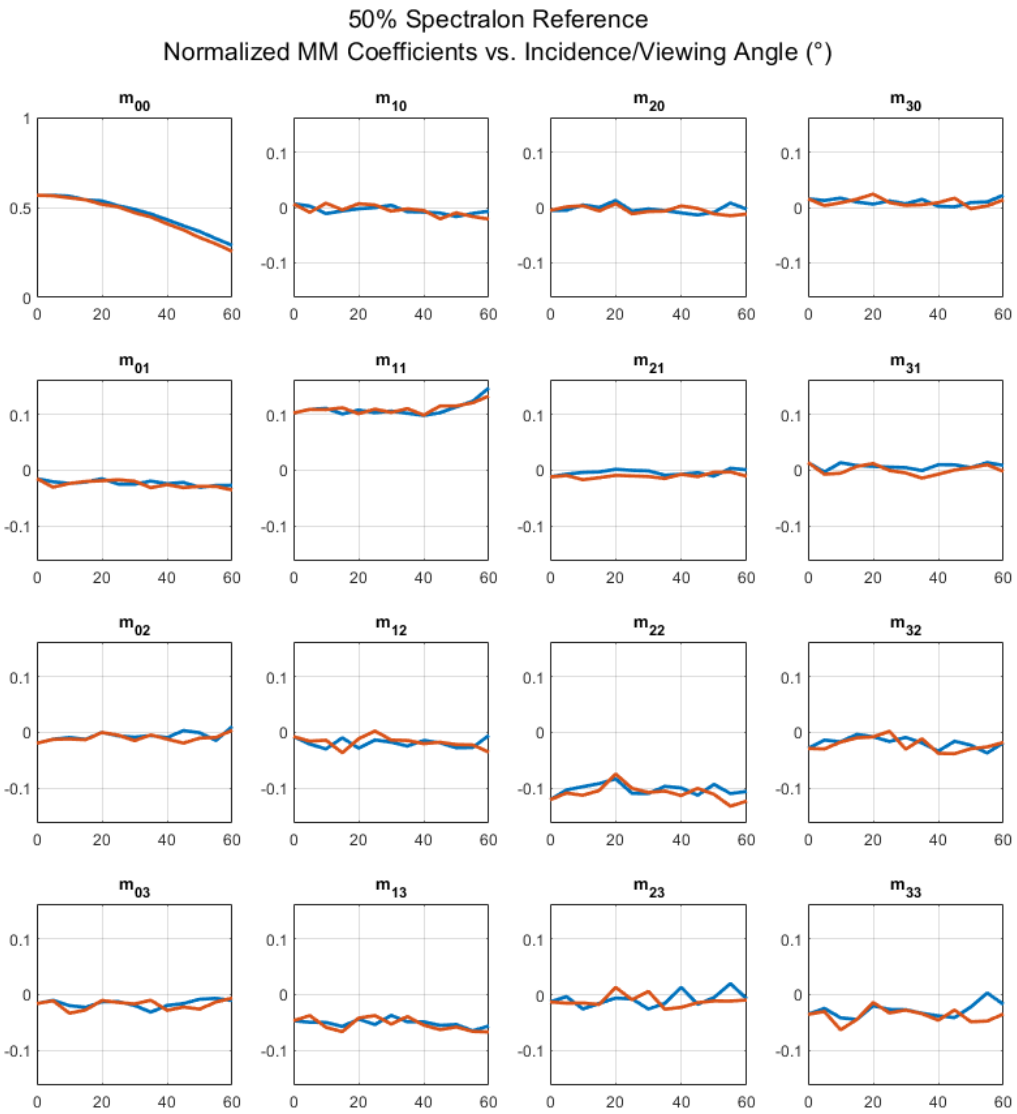

Figure 6. Mueller matrix mBRDF for a 50% Spectralon panel. The blue lines denote negative angles, and the red lines denote positive angles.

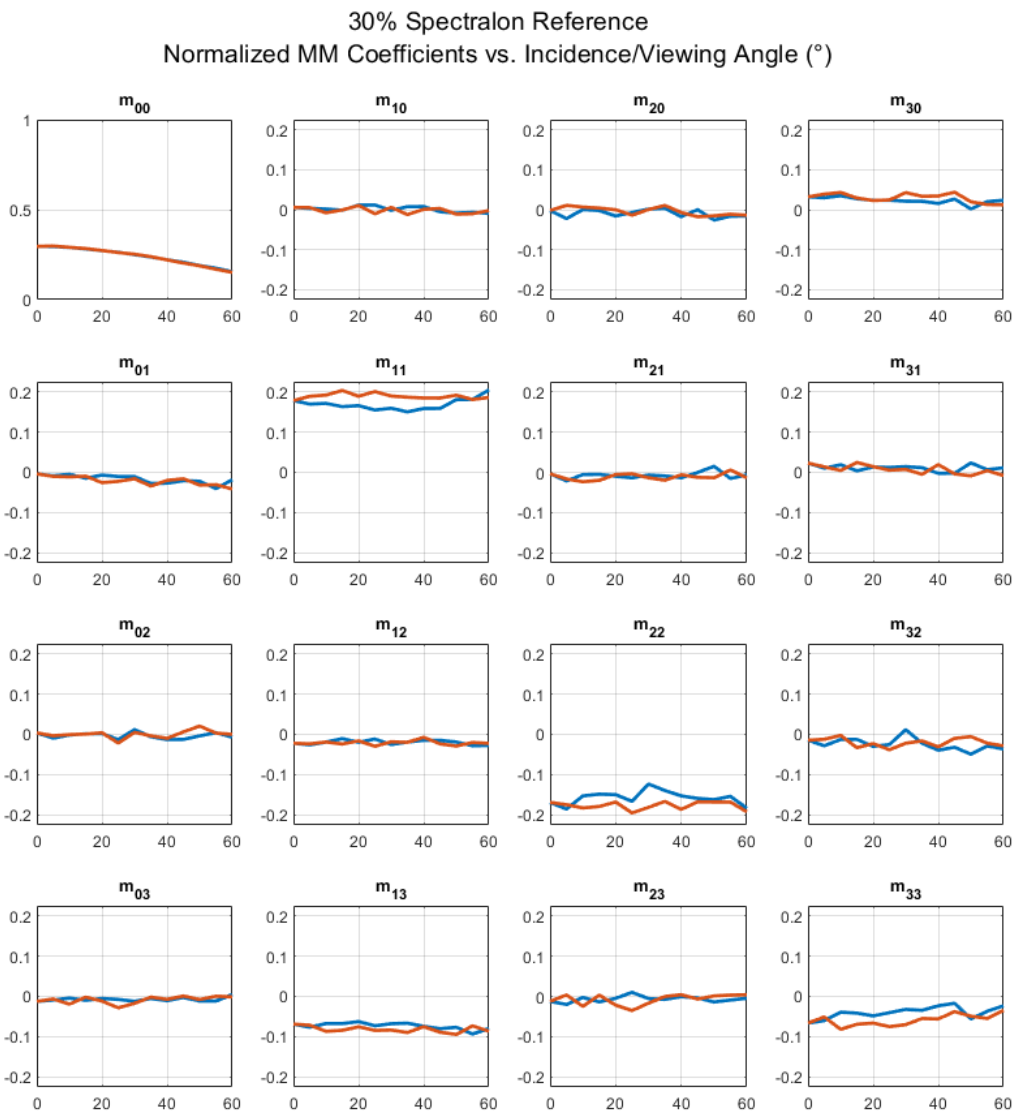

Figure 7. Mueller matrix mBRDF for a 30% Spectralon panel. The blue lines denote negative angles, and the red lines denote positive angles.

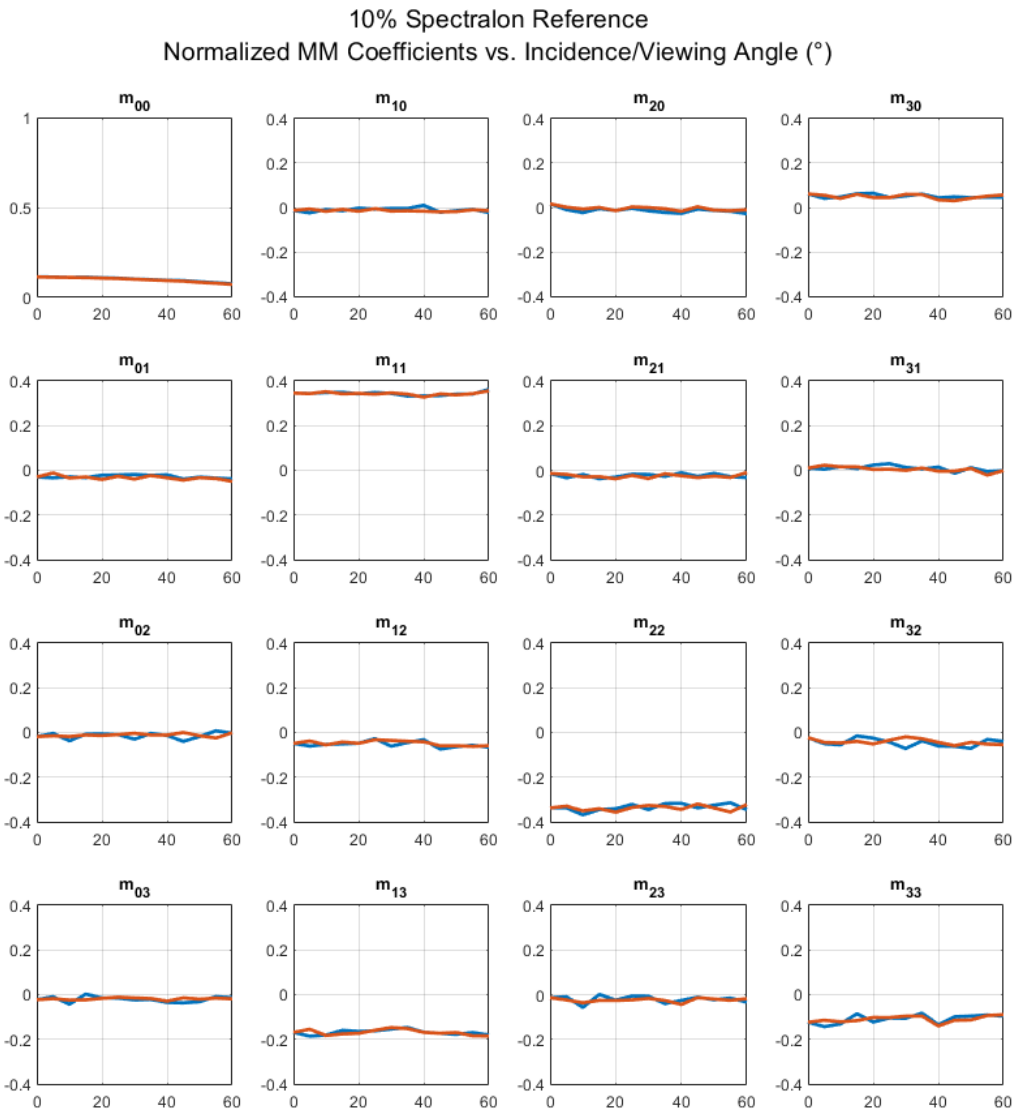

Figure 8. Mueller matrix mBRDF for a 10% Spectralon panel. The blue lines denote negative angles, and the red lines denote positive angles.

One interesting feature of the polarimetric response of the 99% panel is the sharp increase in m_{11} with increasing incidence angle. This represents an increase in maintained vertical and horizontal polarization at steeper incidence/viewing angles. Another notable feature is the reduced magnitude of m_{33} (circular polarization maintenance) as compared with the linear polarization maintenance coefficients (m_{11} and m_{22}). The polarizance (m_{01} and m_{10}) with increasing angle is very weak.

The increase in m_{11} is still present with increasing angle for the 50% panel, and the circular maintenance remains lesser in magnitude than the linear maintenance coefficients. The polarizance is slightly greater for this panel than for the 99% panel. The 30% panel is the first which does not show a strong increase in m_{11} with increasing angle. The circular maintenance is still lesser than the linear maintenance coefficients. The polarizance is greater here, and the darker panels show much stronger maintenance coefficients than the lighter panels. The darkest panel has the strongest polarization maintenance and polarizance. Of additional interest is the lower variance of the measurements for this panel compared to the others.

All of the panels show m_{13} coefficients of significantly greater magnitude than the other off-diagonal components, suggesting some birefringence. However, we have not yet been able to fully verify our polarimeter's circular measurements, so these results are only preliminary.

A final feature not mentioned previously is the polarizance as a function of panel reflectivity. As noted in Fig. 8, the polarizance is seen to increase with decreasing panel reflectance. This is consistent with previous findings [1,11].

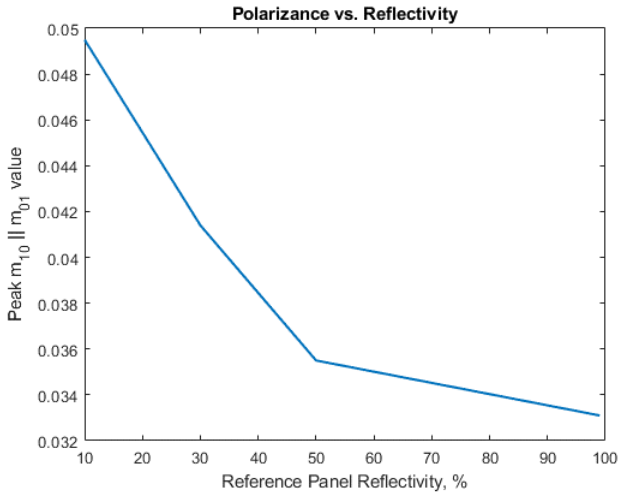

Figure 9. Plot of polarizance vs. nominal panel reflectance.

4. Summary and Conclusions

The MSU Mueller lidar test-bed and the AFRL TMP-LADAR both show similar qualitative deviations in mBRDF from an ideal Lambertian surface. Interestingly, darker panels' mBRDF deviate from the ideal less than brighter panels'. Moreover, there is a clear trend for brighter panels to have lower mBRDF than ideal with increasing angle, while darker panels have higher mBRDF than ideal with increasing angle. This study also validated the use of a reference method for BRDF measurements which avoids the direct measurement of transmitter output.

As for polarization characteristics, we noted increasing polarization maintenance with darker panels and reduced circular polarization maintenance as compared to linear maintenance for all panels. We also saw an increase in vertical/horizontal maintenance (m_{11}) with increasing angle for brighter panels, though this characteristic disappeared as the panels got darker. The expected increase in polarizance for darker panels was also observed.

Acknowledgements

This work was completed as fundamental research in conjunction with research funded by the AFRL as part of a contract with S2 Corporation in Bozeman, MT.

References

1. D. H. Goldstein, D. B. Chenault, and J. L. Pezzaniti, "Polarimetric characterization of Spectralon," Polarization: Measurement, Analysis, and Remote Sensing II **3754**(October 1999), 126–136 (1999).
2. E. M. Rollin, D. R. Emery, and E. J. Milton, "Reference panel anisotropy and diffuse radiation - some implications for field spectroscopy," International Journal of Remote Sensing **21**(15), 2799–2810 (2000).
3. A. Shaw, M. G. Daly, E. Cloutis, G. Basic, D. Hamilton, K. Tait, B. Hyde, E. Lymer, and K. Balachandran, "Reflectance properties of grey-scale Spectralon® as a function of viewing angle, wavelength, and polarization," International Journal of Remote Sensing **37**(11), 2510–2523 (2016).
4. A. Bhandari, B. Hamre, Ø. Frette, L. Zhao, J. J. Stamnes, and M. Kildemo, "Bidirectional reflectance distribution function of Spectralon white reflectance standard illuminated by incoherent unpolarized and plane-polarized light," Applied Optics **50**(16), 2431–2442 (2011).
5. Ø. Svensen, M. Kildemo, J. Maria, J. J. Stamnes, and Ø. Frette, "Mueller matrix measurements and modeling pertaining to Spectralon white reflectance standards," Optics Express **20**(14), 15045 (2012).
6. T. A. Germer, "Full four-dimensional and reciprocal Mueller matrix bidirectional reflectance distribution function of sintered polytetrafluoroethylene," Appl. Opt. **56**(33), 9333–9340 (2017).
7. G. T. Georgiev and J. J. Butler, "BRDF study of gray-scale Spectralon," in *Earth Observing Systems XIII* (SPIE, 2008), **7081**, p. 708107.
8. A. Parretta and M. L. Addonizio, "Optical and Structural Characterization of Diffuse Reflectance Standards Light backscattered from textured surfaces View project Optical and Structural Characterization of Diffuse Reflectance Standards," International Journal of Optics and Applications **5**(2), 33–49 (2015).
9. C. J. Bruegge, A. E. Stiegman, R. A. Rainen, and A. W. Springsteen, "Use of Spectralon as a diffuse reflectance standard for in-flight calibration of earth-orbiting sensors," Optical Engineering **32**(4), 805 (1993).
10. C. Keyser, K. Nguyen, A. Adams, and R. Martin, "Single-pulse mueller matrix polarimeter laboratory demonstration," RAPID 2018 - 2018 IEEE Research and Applications of Photonics In Defense Conference (4), 181–184 (2018).
11. N. J. Field, M. R. Roddewig, and J. A. Shaw, "Near-monostatic angular Mueller matrix measurements using a simple laser polarimeter," in *Polarization Science and Remote Sensing X*, M. K. Kupinski, J. A. Shaw, and F. Snik, eds. (SPIE, 2021), **11833**, pp. 175 – 185.